Journal of Cell Science 113, 3509-3517 (2000)
Printed in Great Britain © The Company of Biologists Limited 2000
JCS4695

Isoforms of caveolin-1 and caveolar structure

Toyoshi Fujimoto[1,*], Hiroshi Kogo[1], Ryuji Nomura[1] and Tomoko Une[2]

[1]Department of Anatomy and Molecular Cell Biology, Nagoya University Graduate School of Medicine, Nagoya 466-8550, Japan
[2]Department of Anatomy, Gunma University School of Medicine, Maebashi 371-8511, Japan
*Author for correpondence (e-mail: tfujimot@med.nagoya-u.ac.jp)

Accepted 13 July; published on WWW 13 September 2000

SUMMARY

The relationship between caveolin-1 isoforms (α and β) and caveolar ultrastructure was studied. By immunofluorescence microscopy of human fibroblasts, caveolae were observed as dots positive for caveolin-1, but many dots labeled by an antibody recognizing both isoforms (anti-αβ) were not labeled by another antibody specific for the α isoform (anti-α). Immunogold electron microscopy of freeze-fracture replicas revealed caveolae of different depths, and indicated that anti-α labeled deep caveolae preferentially over shallow ones, whereas anti-αβ labeled both forms with an equivalent frequency and intensity. The presence of the β isoform in deep caveolae was confirmed by labeling epitope-tagged β-caveolin. When made to be expressed in HepG2 cells lacking endogenous caveolins, the α isoform formed caveolar depressions efficiently, but the β isoform hardly did so. Caveolae were also formed in cells expressing the two isoforms, but their frequency was variable among cells of the same clone. Coexpression of caveolin-1 and caveolin-2 caused more efficient formation of deep caveolae than caveolin-1 alone. The result indicates that the two isoforms of caveolin-1 have a different potential for forming caveolae structure, and more importantly, that deep and shallow caveolae may be diversified in their molecular composition.

Key words: Caveolae, Caveolin-1, Isoform, Freeze-fracture, Caveolin-2

INTRODUCTION

Caveolae are small invaginations of the cell surface and are thought to play a role in important physiological functions such as cell surface signaling, endocytosis and intracellular cholesterol transport (for reviews, see Parton, 1996; Anderson, 1998; Fujimoto et al., 1998). Unique membrane proteins named caveolin-1, -2, and -3 have been shown to be major constituents of caveolae (Rothberg et al., 1992; Scherer et al., 1996; Tang et al., 1996). Among them, caveolin-1 was discovered first and has been characterized most extensively. The protein is assumed to take a hairpin-loop conformation in the lipid bilayer, thereby exposing both the N and C termini to the cytoplasmic surface (Parton, 1996). A stretch of amino acids referred to as the scaffolding domain interacts with many signaling proteins (Li et al., 1996a), and caveolin-1 can bind to cholesterol. This latter property appears to be related to the unique lipidic composition of the caveolar membrane and intracellular cholesterol transport (Murata et al., 1995; Smart et al., 1996). Furthermore, expression of caveolin-1 led to de novo formation of caveolae (Fra et al., 1995). These observations suggest that caveolin-1 is an indispensable protein for both the structure and function of caveolae.

Caveolin-1 is expressed in two isoforms, caveolin-1α and caveolin-1β; the α and β isoforms start from methionine at positions 1 and 32, respectively (Scherer et al., 1995). Thus the two isoforms have in common a hydrophobic stretch of amino acids, the scaffolding domain, and the acylated C-terminal region, whereas the N-terminal 31 amino acids are only found in the α isoform. The two isoforms were reported to show an overlapping but slightly different distribution in mammalian cells (Scherer et al., 1995), and to induce a homogeneous population of vesicles in insect cells (Li et al., 1996b), but no detailed study concerning their functional diversity has been performed.

Caveolae were originally defined morphologically as smooth plasmalemmal invaginations of round flask shape (Yamada, 1955), but it was later found by quick-freeze deep-etch electron microscopy that a unique striped pattern exists on the cytoplasmic surface, not only in the deep invaginations, or 'classical' caveolae, but also in shallower depressions (Rothberg et al., 1992). The latter structure is also positive for caveolin-1 and is assumed to become a deep invagination. In the present study, we found that the ratio of caveolin-1 isoforms varies in shallow and deep caveolae of human fibroblasts. Furthermore, when the two isoforms were expressed singly or in combination in HepG2 cells lacking endogenous caveolins, de novo formation of caveolae occurred in different manners and efficiency. Our result indicates that the α and β isoform of caveolin-1 have different potentials in caveola formation and that the molecular composition of caveolae may not be the same; it also suggests that caveolae of different depths may be generated by a mechanism distinct from that of clathrin-coated pits.

MATERIALS AND METHODS

Cells

Human fibroblasts were explanted from biopsied normal human adult skin. CHO and HepG2 cells were obtained from the Japanese Cancer Research Resources Bank (Tokyo, Japan). The cells were grown in DME (Nihonseiyaku Co., Tokyo) supplemented with 10% fetal bovine serum (FBS), 50 U/ml penicillin, and 0.05 mg/ml streptomycin at 37°C in 5% CO_2. They were cultured on glass coverslips for immunofluorescence microscopy and on thin gold foil for immunoelectron microscopy of freeze replicas (Fujimoto and Fujimoto, 1997).

Antibodies

Anti-caveolin-1 antibodies used were: rabbit polyclonal anti-caveolin-1 antibodies (C13630: Transduction Lab., Lexington, KY, USA; sc-894: Santa Cruz Biotechnology, Inc., Santa Cruz, CA, USA) and mouse monoclonal anti-caveolin-1 antibodies (clone Z034: Zymed Lab., Inc., South San Francisco, CA, USA; clones 2297 and 2234: Transduction Lab.). Mouse anti-caveolin-2 antibody (Transduction Lab.), rabbit anti-HA.11 antibody (Berkeley Antibody Co., Richmond, CA, USA), mouse anti-HA antibody (12CA5, Boehringer-Mannheim Corp., Indianapolis, IN, USA), fluorescein- and rhodamine-conjugated donkey antibodies (Jackson ImmunoResearch Lab., West Grove, PA, USA), and colloidal gold-conjugated goat antibodies (Amersham, Buckinghamshire, UK) were also used.

Caveolin cDNAs and transfection

The codon of methionine at position 32 in human α-caveolin-1 cDNA was changed to code for leucine (ATG to TTG) by use of a QuikChange Site-Directed Mutagenesis Kit (Stratagene, Inc., La Jolla, CA, USA). The cDNA encoding human β-caveolin-1, either as such or tagged with the HA epitope (9 amino acids: YPYDVPDYA) at the C terminus, were subcloned into pcDNA3.1(+) (Invitrogen, San Diego, CA, USA) and used to transfect to CHO and HepG2 cells by lipofection. In one experiment, HepG2 cells were transfected simultaneously with the cDNAs of human caveolin-1 and caveolin-2. Stably transfected cell lines were selected with G418 (Gibco BRL, Rockville, MD, USA).

Immunoblotting and RT-PCR

Total lysates of cultured cells were separated by SDS-PAGE in 12% or 15% acrylamide gels, electrotransferred to nitrocellulose paper and probed with antibodies to caveolins. After incubation with horseradish peroxidase-conjugated secondary antibodies, the reaction was visualized by use of the SuperSignal ULTRA Chemiluminescent substrate (Pierce) as instructed by the manufacturer.

cDNA was synthesized by a SuperScript preamplification system from total RNA extracted with TRIZOL reagent (Gibco BRL). PCR was performed by using forward and reverse primers synthesized according to published cDNA sequences of caveolin-1, -2, and -3 (GenBank accession numbers: Z18951, U32114 and U31968, respectively), and products were electrophoresed in 2% agarose gels and stained by ethidium bromide.

Immunofluorescence microscopy

The basal plasma membrane of human fibroblasts were obtained as described previously (Fujimoto et al., 1991). Briefly, the cells were washed three times with PBS, rinsed once with the cytosol buffer (20 mM Pipes-NaOH, 100 mM KCl, 5 mM $MgCl_2$, 3 mM EGTA, pH 6.8), rinsed once with the cytosol buffer diluted 1/3, and overlaid with prewet nitrocellulose paper. The upper half of the cells was removed by peeling off the paper, and the remaining membrane was immediately fixed with 3% formaldehyde in phosphate-buffered saline (PBS) for 5 minutes. The intact cell was also fixed by the same fixative or by methanol at –20°C.

The fixed samples were treated with 1% bovine serum albumin (BSA), incubated with a mixture of rabbit anti-caveolin-1 (C13630; 0.5 μg/ml) and mouse anti-caveolin-1 (clone 2234; 12.5 μg/ml) antibodies for 60 minutes, and then with a mixture of fluorescein-conjugated donkey anti-rabbit IgG antibody (20 μg/ml) and rhodamine-conjugated donkey anti-mouse antibody (20 μg/ml) for 60 minutes. In some experiments, fluorochromes for the two antibodies were exchanged. All the steps were done on ice.

Photomicrographs were taken on Kodak T-max 400 film by a Zeiss Axiophot2 microscope. The images were input into an Apple Power Macintosh computer through a film scanner and artificially colored using IPLab (Scanalytics, Inc., Fairfax, VA, USA).

Immunoelectron microscopy

Cells were rapidly frozen by the metal sandwich method (Fujimoto and Fujimoto, 1997). They were freeze-fractured in Balzers BAF401 and BAF060 apparatuses (Balzers High Vacuum Corp., Balzers, Liechtenstein), and the obtained platinum/carbon replicas were digested with SDS, treated with BSA for blocking, and then incubated with rabbit or mouse anti-caveolin-1 and anti-caveolin-2 antibodies (0.5-20 μg/ml) (Fujimoto, 1995). They were further incubated with 10-nm colloidal gold-conjugated goat anti-rabbit IgG or anti-mouse IgG antibodies (diluted to 1/30) and observed under a JEOL 100CX electron microscope.

To quantify the immunogold labeling, we chose cells randomly and printed the pictures at about ×20,000. For human fibroblasts, gold particles directly in contact with deep caveolae and those within the perimeter of shallow caveolae were counted. For HepG2 cells, gold labeling existing as a cluster of more than 3 particles was selected, and associated structures were counted.

Oligomerization of caveolin-1

Oligomer formation of caveolin-1 in transfected HepG2 cells was examined according to the published protocol (Sargiacomo et al., 1995) with some modifications. Briefly, the Triton X-100-insoluble pellet was treated with a lysis buffer (1% Triton X-100, 60 mM octylglucoside, 25 mM 2-(*N*-morpholino)ethanesulfonic acid, 150 mM NaCl, 1 mM (*p*-amidinophenyl)methanesulfonyl fluoride hydrochloride, 1 mM sodium orthovanadate, pH 6.5) for 20 minutes on ice and centrifuged at 100,000 ***g*** for 30 minutes. The supernatant was layered onto a 5%-30% linear sucrose gradient in the lysis buffer, and centrifuged in a SW41 rotor at 100,000 ***g*** for 20 hours at 4°C. Fractions were collected, precipitated with cold acetone, and analyzed by western blotting.

RESULTS

Antibodies

Five different antibodies were used to detect caveolin-1. Specific for the α isoform (called anti-α hereafter) were: one polyclonal (sc-894) and one monoclonal (clone 2234) antibody; and recognizing both α and β isoforms (anti-αβ) were: one polyclonal (C13630) and two monoclonal (clones 2297 and Z034) antibodies (Fig. 1). In western blotting of human fibroblasts, clones 2297 and Z034 bound to the two isoforms with equal intensity, whereas C13630 reacted with the α isoform better than with the β isoform. The different reaction intensity was also observed with other cell lysates.

Immunolabeling of human fibroblasts

When human fibroblasts were fixed as whole cells and doubly labeled with anti-α and anti-αβ antibodies, the labeling by the two antibodies appeared the same (not shown). When the basal plasma membrane preparation was labeled by the same

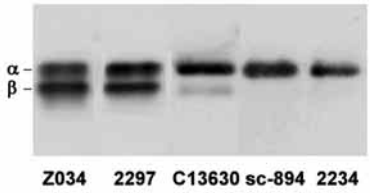

Fig. 1. Western blotting of caveolin-1 isoforms by five different anti-caveolin-1 antibodies used in the present experiment. Human fibroblast lysate was electrophoresed and electrotransferred. Note that one anti-αβ antibody (C13630) recognized the α isoform more efficiently than the β isoform.

antibodies, the labeling was seen as a collection of small dots, and the general distribution appeared similar for the two antibodies (Fig. 2a-c). The diameter of each fluorescent dot was 250-500 nm, about 5 times of the diameter of a caveola, but considering the size of the antibodies and the characteristics of fluorescent images, each dot is likely to correspond to a single caveola. At higher magnification, a significant number of dots was labeled by anti-αβ alone, and not by anti-α (Fig. 2d-f). Naturally dots labeled by anti-α but not by anti-αβ were few. The result did not change whether the anti-α and anti-αβ were applied simultaneously or sequentially, or when fluorochromes for the antibodies were exchanged. Thus competition between the two antibodies, different film sensitivity of fluorochromes, or bleaching of fluorescence were not involved. This result indicates the presence of two kinds of caveolae, which are different in their composition of caveolin-1 isoforms.

Fine distribution of the labeling was examined by using freeze-fracture replicas. Two kinds of invaginations were

Table 1. Immunogold labeling associated with deep and shallow caveolae in human fibroblast

Antibodies	Percentage of labeled caveolae		Average number of gold particles per caveola		Deep/shallow ratio
	Deep caveolae	Shallow caveolae	Deep caveolae	Shallow caveolae	
Anti-caveolin-1α					
sc-894	99.4	62.1	4.97±2.20	1.00±1.08	4.97
Clone 2234	54.6	4.7	0.93±1.11	0.05±0.25	18.6
Anti-caveolin-1αβ					
C13630	100.0	96.6	7.90±1.81	3.42±1.75	2.31
Clone 2297	99.3	97.4	7.26±2.23	4.53±2.18	1.60
Clone Z034	99.1	98.8	6.41±2.18	3.88±1.93	1.65
Anti-caveolin-2					
Clone 65	96.7	84.9	3.76±1.96	2.53±1.92	1.49

Freeze-fracture replicas of human fibroblasts were labeled by different antibodies. The frequency of labeling and the number of gold particles for deep and shallow caveolae were measured.

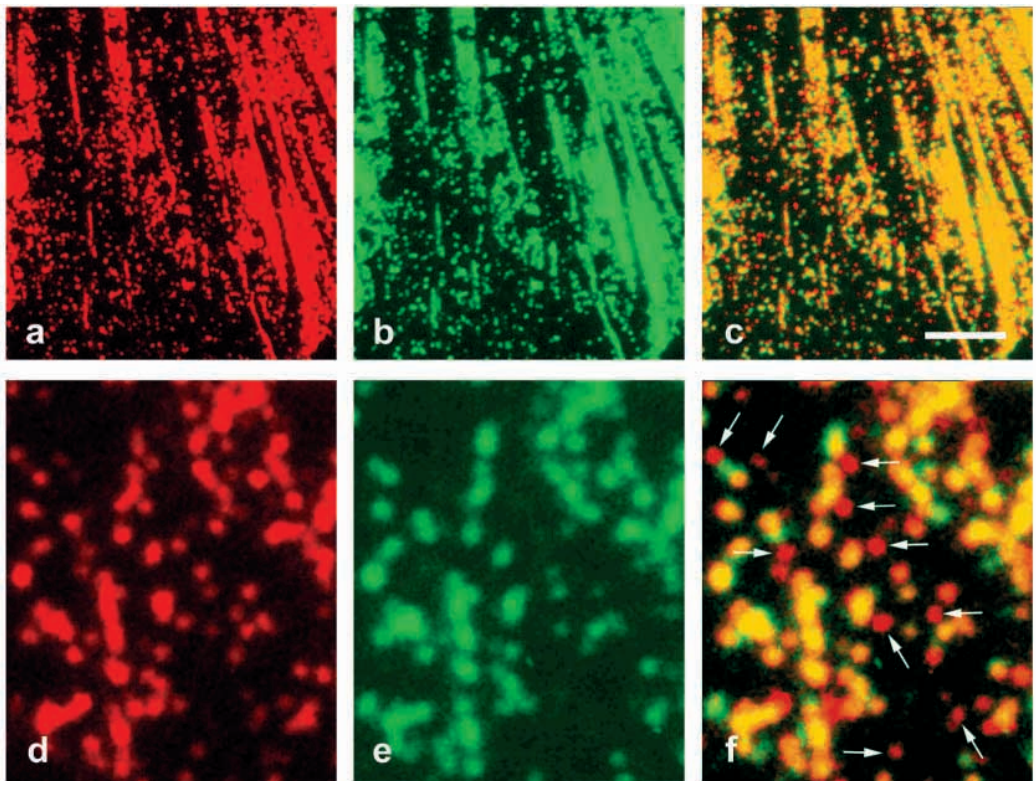

Fig. 2. Immunofluorescence microscopy of caveolin-1. The ventral membrane of human fibroblasts was doubly labeled by anti-αβ (a,d: red) and anti-α (b,e: green) antibodies. Figs 2c and 2f are merged images. The general distribution of the labeling appears similar for the two antibodies (a-c); but at a higher magnification, there are many dots that are labeled by anti-αβ, but not by anti-α (arrows) (d-f). Bar, 1 μm (a-c), 4.3 μm (d-f).

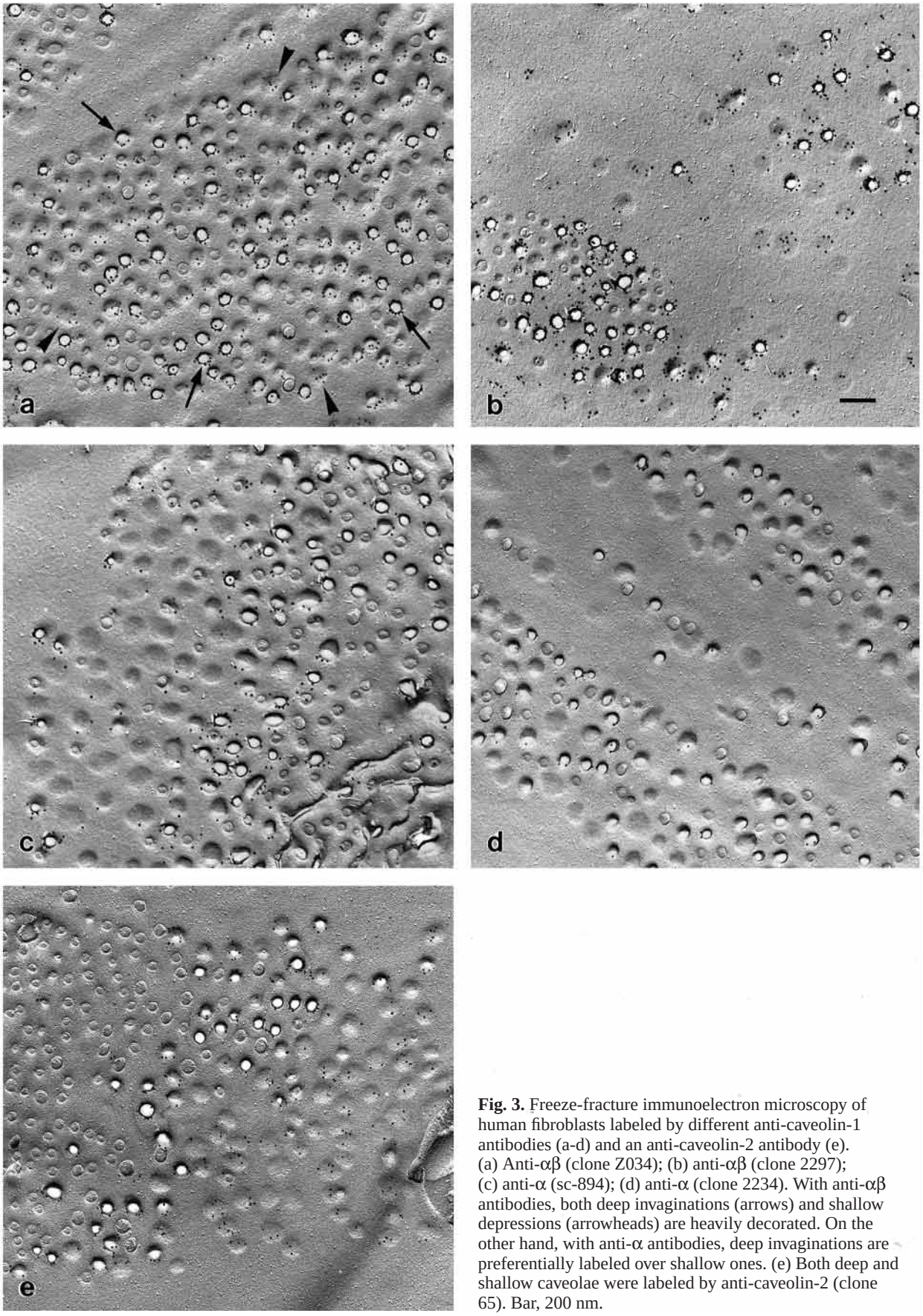

Fig. 3. Freeze-fracture immunoelectron microscopy of human fibroblasts labeled by different anti-caveolin-1 antibodies (a-d) and an anti-caveolin-2 antibody (e). (a) Anti-αβ (clone Z034); (b) anti-αβ (clone 2297); (c) anti-α (sc-894); (d) anti-α (clone 2234). With anti-αβ antibodies, both deep invaginations (arrows) and shallow depressions (arrowheads) are heavily decorated. On the other hand, with anti-α antibodies, deep invaginations are preferentially labeled over shallow ones. (e) Both deep and shallow caveolae were labeled by anti-caveolin-2 (clone 65). Bar, 200 nm.

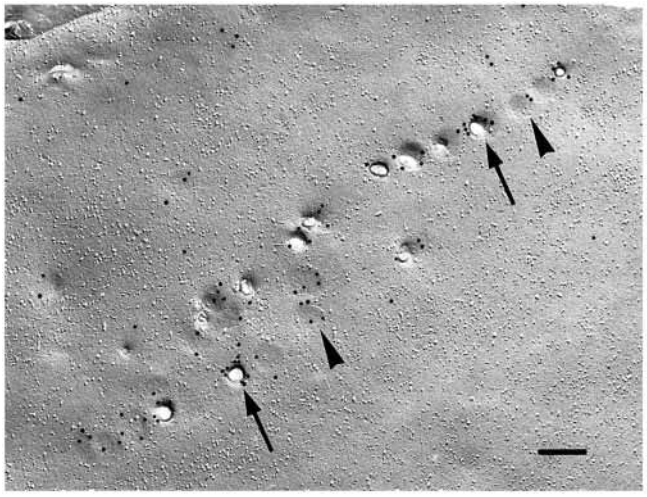

Fig. 4. Freeze-fracture immunoelectron microscopy of CHO cells transfected with cDNA of HA-tagged caveolin-1β. The labeling for HA is seen in both deep (arrows) and shallow caveolae (arrowheads). Bar, 200 nm.

observed in the replicas (Fig. 3a-d): deep ones were fractured at the neck and their bottom appeared white because of the paucity of platinum shadowing; on the other hand, shallow ones were fractured and replicated along their whole contour. Others appearing as craters were not labeled. By use of three different anti-αβ antibodies, virtually all the deep and shallow invaginations were labeled positively, and few gold particles were seen in the non-invaginated membrane (Fig. 3a,b). On the other hand, with the two anti-α antibodies, a majority of deep invaginations were labeled, but shallow ones were far less so (Fig. 3c,d). Localization of caveolin-2, which forms a heteropolymer with caveolin-1 (Scherer et al., 1997), was also examined; it was labeled equally well in both deep and shallow invaginations (Fig. 3e). Since invaginations were shown to be positive for caveolins irrespective of their depth, they are hereafter termed collectively as caveolae. By quantifying the immunolabeling results, significant differences were seen between anti-α and anti-αβ antibodies, both in the percentage of labeled caveolae and in the number gold particles per caveola (Table 1); reasonably, C13630, which binds to the α isoform better than to the β isoform in western blotting (Fig. 1), showed an intermediate result between the two groups. In conjunction with the immunofluorescence results, these data indicate that there are two populations of caveolae and that the α to β ratio of caveolin-1 isoforms (α/β) is higher in deep caveolae than in shallow ones.

CHO cells expressing HA-tagged caveolin-1β

The results on human fibroblasts showed a diversity of the isoform ratio among caveolae, but due to the lack of an antibody specific for the β isoform, we could not determine whether some caveolae consist of the α isoform alone. To answer this question, we transfected CHO cells with cDNA of human caveolin-1β tagged with the HA epitope, and observed its localization by immunohistochemistry. CHO cells express both α and β isoforms of endogenous caveolin-1. By double-labeling immunofluorescence microscopy using rabbit anti-α (sc-894) and mouse anti-HA antibodies, the general distribution was the same (not shown). By immunoelectron microscopy of freeze replicas, the labeling for HA was seen in both deep and shallow caveolae (Fig. 4). This result indicates that the β isoform is present in both of them.

Table 2. Plasmalemmal structures labeled for caveolin-1 in transfected HepG2 cell

	Deep invagination	Shallow depression	No differentiation
HepG2-α			
Clone 1	7.9%	57.6%	39.1%
Clone 2	13.9%	69.9%	16.2%
HepG2-β			
Clone 1	0.56%	5.1%	94.4%
Clone 2	0.50%	6.3%	93.1%
HepG2-αβ			
Clone 1	0%	47.3%	52.7%
Clone 2	0.80%	50.0%	49.2%
HepG2-αβ+2			
Clone 1	20.7%	21.3%	58.0%

Stable clones were examined for the four cell types: HepG2-α, HepG2-β, HepG2-αβ, and HepG2-αβ+2. Freeze-fracture replicas were labeled by anti-caveolin-1αβ or by anti-caveolin-2 antibody and structures associated with a cluster of more than three gold particles were counted.

HepG2 cells expressing α isoform alone, β isoform alone, or both α and β isoforms

For further elucidation of the difference between the two isoforms, HepG2 cells, which do not express caveolins endogenously, were transfected with cDNA of either the α isoform alone, β isoform alone, or both α and β isoforms of human caveolin-1, and formation of caveolae was examined. The lack of caveolins in HepG2 cells was confirmed by RT-PCR (Fig. 5a) and western blotting (Fig. 5b and data not shown). To obtain the expression of the α isoform alone, we altered the cDNA of α-caveolin-1 by replacing the methionine at position 32 with leucine. For the expression of both α and β isoforms, native cDNA of caveolin-1 was used for transfection, and generation of the two isoforms was confirmed by western blotting (Fig. 5b).

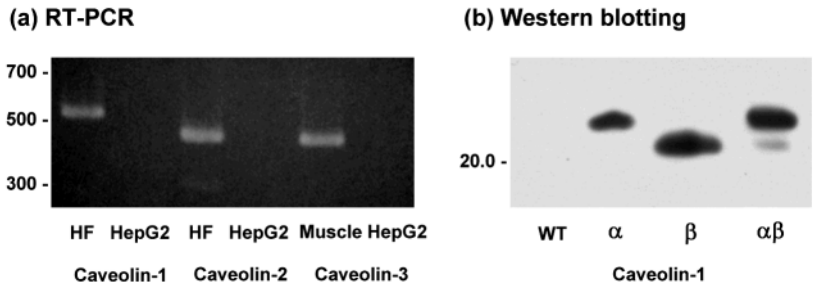

Fig. 5. (a) The absence of caveolins in wild-type HepG2 shown by RT-PCR. Total RNA obtained from human fibroblasts (HF) and mouse skeletal muscle cells (muscle) were used as positive controls. (b) Western blotting of wild-type HepG2 (WT), HepG2-α (a), HepG2-β (b) and HepG2-αβ (αβ) with anti-caveolin-1αβ antibody. Isoforms of caveolin-1 are expressed in the three clones as expected.

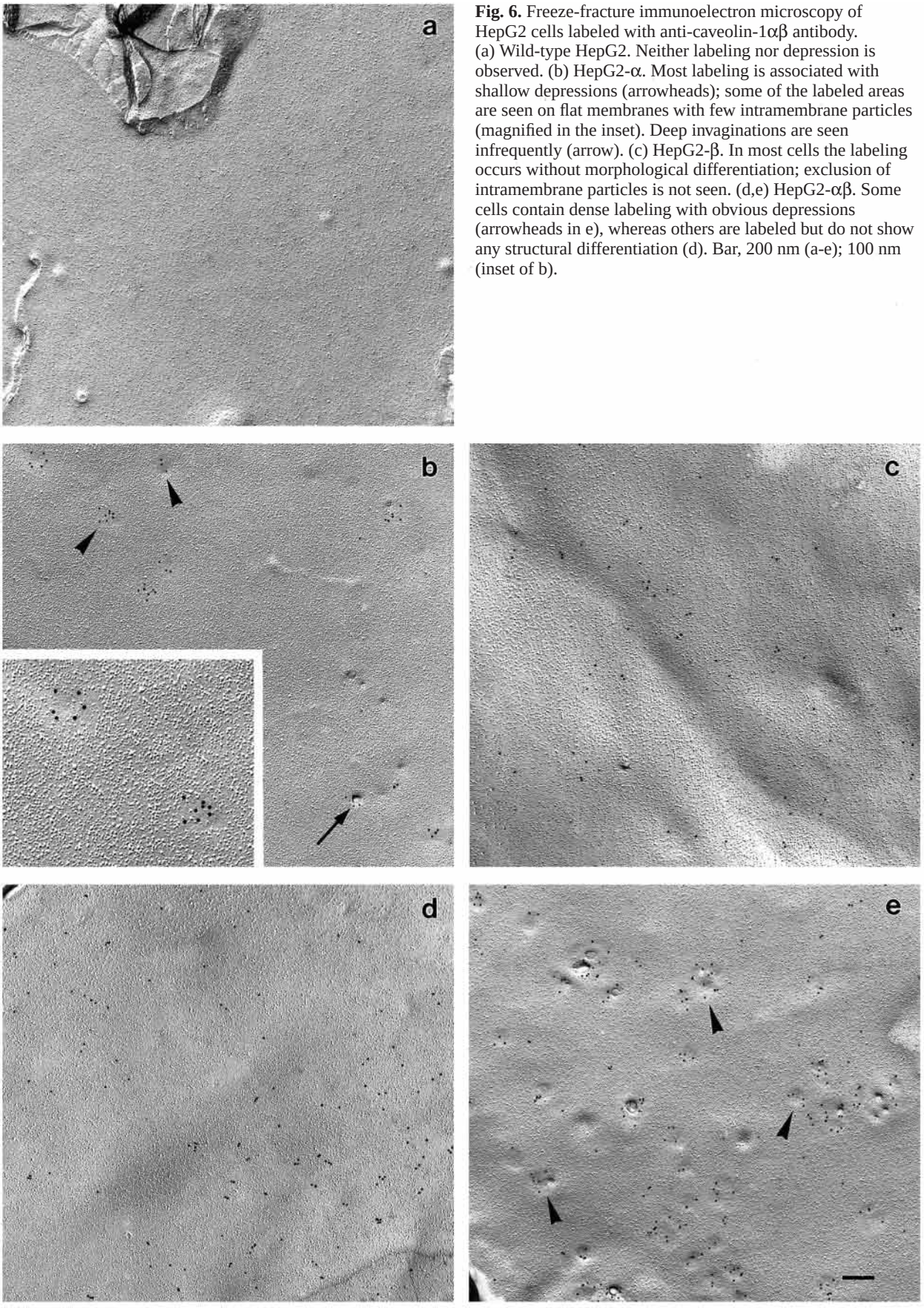

Fig. 6. Freeze-fracture immunoelectron microscopy of HepG2 cells labeled with anti-caveolin-1αβ antibody. (a) Wild-type HepG2. Neither labeling nor depression is observed. (b) HepG2-α. Most labeling is associated with shallow depressions (arrowheads); some of the labeled areas are seen on flat membranes with few intramembrane particles (magnified in the inset). Deep invaginations are seen infrequently (arrow). (c) HepG2-β. In most cells the labeling occurs without morphological differentiation; exclusion of intramembrane particles is not seen. (d,e) HepG2-αβ. Some cells contain dense labeling with obvious depressions (arrowheads in e), whereas others are labeled but do not show any structural differentiation (d). Bar, 200 nm (a-e); 100 nm (inset of b).

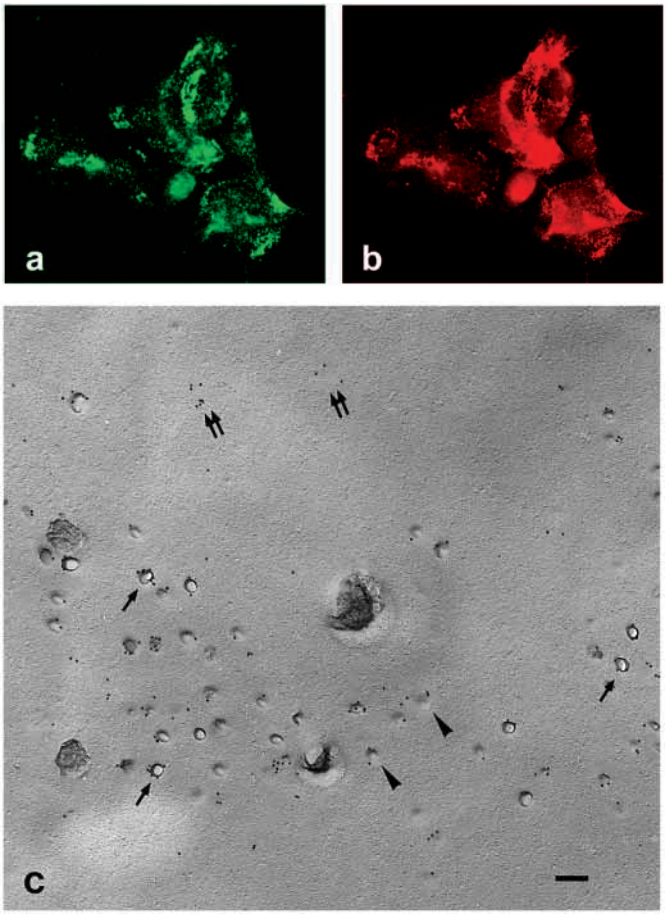

Fig. 7. HepG2 cells expressing α and β isoforms of caveolin-1 and caveolin-2 (HepG2-αβ+2). (a) Immunofluorescence microscopy. Caveolin-1 and -2 are localized in the same patches on the cell surface. (b) Freeze-fracture immunoelectron microscopy. The labeling for caveolin-2 is seen either associated with deep (single arrow) and shallow (arrowhead) caveolae, or with flat membrane areas (double arrows). Bars, 10 μm (a); 200 nm (b).

To assess the potential of caveolin-1 isoforms for forming the caveolar structure, stable clones from each experimental group were examined by freeze-fracture immunoelectron microscopy using an anti-αβ antibody (clone 2297) (Fig. 6); the result was quantitated by measuring the frequency of structures associated with clusters of more than three gold particles (Table 2). Wild-type HepG2 cells did not show any labeling or depressions indicative of caveolae (Fig. 6a). In cells transfected with cDNA of the α isoform alone (HepG2-α), gold particles were observed in clusters; and a majority of them were associated with shallow depressions (Fig. 6b); the labeled areas sometimes appeared to be nearly flat, but they were demarcated by exclusion of intramembrane particles (inset of Fig. 6b). Deep invaginations were also present, but only infrequently. In most cells expressing the β isoform alone (HepG2-β), gold particles were also found in clusters, but most of them were seen on membrane areas without any visible differentiation (Fig. 6c). In a few cells the label was associated with shallow depressions (not shown). The divergent result was not apparently due to a difference in the labeling density.

In cells expressing both α and β isoforms (HepG2-αβ), about half of the label was present on flat undifferentiated membrane (Fig. 6d), whereas the rest was associated with shallow depressions (Fig. 6e). Nonuniformity among cells in the same clone also occurred in HepG2-αβ: most labeling was associated with depressions in some cells, whereas it was not so in other cells. To exclude the possibility that segregated expression of α and β isoforms occurred among HepG2-αβ cells and thus caused the heterogeneous result in a clone, we also labeled replicas with an anti-α antibody (sc-894), but the result was essentially the same as with the anti-αβ antibody (result not shown).

The effect of caveolin-2 on the caveolae formation was examined in cells expressing both caveolin-1 (both α and β isoforms) and caveolin-2 (HepG2-αβ+2). By double immunofluorescence labeling, colocalisation of caveolin-1 and caveolin-2 was apparent (Fig. 7a). Immunoelectron microscopy was done by anti-caveolin-2; the positive labeling ensures that both caveolin-1 and caveolin-2 are expressed in the particular cell because caveolin-2 is trafficked to the plasma membrane only when coexpressed with caveolin-1 (Mora et al., 1999; Parolini et al., 1999). The result was similar to that of HepG2-αβ in that about half of the labeling was on the flat membrane. Nonuniformity in the same clone was also observed. However, the proportion of deep caveolae was much higher than that of HepG2-αβ cells (Fig. 7b, Table 2).

Oligomers of caveolin-1 are supposed to be basic units of caveolae formation. To test whether the above results were caused by different oligomerization potentials of α and β isoforms, we obtained Triton X-100-insoluble materials from HepG2-α, HepG2-β and HepG2-αβ and examined them for large molecular complexes. By density gradient ultracentrifugation, caveolin-1 from the three cell lines was shown to form a complex of similar size (150-400 kDa) (Fig. 8), which was the same as the result reported for insect cells (Li et al., 1996b).

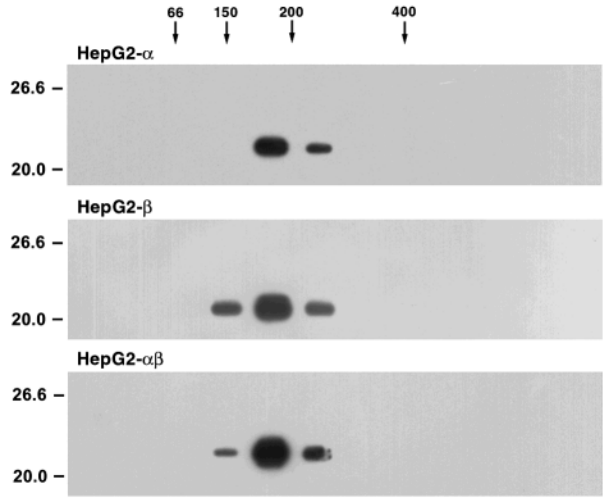

Fig. 8. Oligomer formation of caveolin-1 in HepG2-α, HepG2-β, and HepG2-αβ. Triton X-100-insoluble material was fractionated by sucrose density-gradient centrifugation and immunoblotted with anti-caveolin-1αβ. Arrows mark the positions of the molecular mass standards. Caveolin-1 molecules were detected in the 150-400 kDa range in extracts of all of the cell lines.

DISCUSSION

The α and β isoforms of caveolin-1 were reported to show distinct, but overlapping distribution (Scherer et al., 1995). Although expression of either isoform was shown to generate small intracellular vesicles in insect cells (Li et al., 1996b), whether it could lead to formation of plasmalemmal caveolae has not been studied. The present experiment examined the morphological potential of the two isoforms in mammalian cells. Freeze-fracture immunoelectron microscopy of human fibroblasts inferred the α/β ratio to be higher in the deep caveolae than in the shallow ones. Because molecules retained in the replica were denatured by SDS (Fujimoto, 1995), it is unlikely that the difference of the labeling density was caused by differential conformational change of caveolin-1 in the two types of caveolae. In addition, the segments of caveolin-1 recognized by the antibodies are hydrophilic (Glenney and Soppet, 1992) and should have little chance to be buried in the lipid bilayer. Thus the divergent labeling in caveolae of different depths is likely to reflect the numerical composition of the two isoforms.

The result obtained with HepG2 expressing different combinations of isoforms agrees with that on human fibroblasts in that the α isoform was more efficient than the β isoform in forming caveolae. But some results obtained in HepG2 cells cannot be explained in the same way as those of human fibroblasts. First, although the α/β ratio was maximum in HepG2-α, most of the caveolae were shallow. Second, caveolin-1-positive membrane areas were not associated with any depression in many HepG2-αβ cells. Third, marked heterogeneity was observed in the formation of depressions among cells of the same clone. How can these differences be interpreted?

Because transfection of lymphocytes with caveolin-1 cDNA led to de novo formation of caveolae (Fra et al., 1995), caveolin-1 has been thought to be a necessary and sufficient factor for the invagination. However, compared with that in cells expressing caveolin-1 endogenously, de novo formation of caveolae in cells transfected with caveolin-1 cDNA was reported to be less efficient and not well correlated with the expression level of caveolin-1 (Vogel et al., 1998). Also in the present results, formation of depressions was not correlated with the density of labeling for caveolin-1. Such disparity is likely to be caused by other factors, a candidate being caveolin-2. In fact, deep caveolae were formed efficiently only in the presence of caveolin-2. The result is consistent with that for MDCK cells, in which the deep invaginations were formed only in the basolateral surface where caveolin-1 and -2 coexisted (Scheiffele et al., 1998). Therefore, it is inferred that cooligomerization of caveolin-1 and -2 is necessary for efficient formation of deep caveolae, and this could explain the predominance of shallow caveolae in HepG2-α.

Even when caveolin-2 was present, however, about half of the labeling was not associated with any depression, and marked heterogeneity among cells persisted. A factor responsible for these might be cholesterol. Endogenous caveolin-1 expression is regulated by a sterol-responsive element, and the quantitative ratio of caveolin-1 and cholesterol is thought to be kept fairly constant (Fielding et al., 1997). In contrast, the ratio of transfected caveolin-1 and cholesterol may be variable because the caveolin-1 synthesis proceeds irrespective of the cholesterol content. Moreover, the plasmalemmal cholesterol content appears variable among cells (Fujimoto et al., 1997), and caveolae are formed only when the cellular cholesterol content is above a threshold level (Hailstones et al., 1998). The ratio of caveolin-1 and cholesterol may need to be within a certain range for caveola formation.

Caveolae were first defined as uncoated, round, flask-shaped invaginations (Yamada, 1955), but based on quick-freeze deep-etch electron microscopy (Rothberg et al., 1992) and immunoelectron microscopy using freeze-fracture replicas (Fujimoto and Fujimoto, 1997, and this study), they were redefined as caveolin-1-positive domains of various curvature (Anderson, 1998). In endothelial cells, caveolae were shown to become vesicles (Schnitzer et al., 1996), and it has been assumed that shallow depressions become invaginated deeply and then bud in a similar manner as clathrin-coated pits. But constituents functionally analogous to clathrin or adaptors have not been found in caveolae. The difference in the α/β isoform ratio of caveolin-1 between the deep and shallow caveolae may indicate a unique molecular mechanism underlying the caveolar shape differentiation. Because the two caveolin-1 isoforms are unlikely to be interconvertible, one possibility is that caveolae of different depths could be entirely different entities. Another possibility is that caveolin-1β/caveolin-2 oligomers in the shallow caveolae may be replaced with caveolin-1α/caveolin-2 oligomers for deeper invagination. Hetero-oligomers of caveolin-1 and -2 are thought to be formed in the Golgi through protein-protein interactions of the membrane-spanning domains (Das et al., 1999). It is intriguing to study whether the composition of caveolin oligomers could be modified even after caveolae formation.

Could there be any functional difference between deep and shallow caveolae? They should share many properties that depend on the presence of caveolins; for example, both of them are likely to show the specialized lipid composition rich in glycosphingolipids and cholesterol, and to contain proteins interacting with caveolins (Couet et al., 1997). However, the different depths may impart some functional specialization for the depressions. For example, only deep caveolae could store some molecules in the lumen, which may be discharged to the cytoplasm as a quantum (Anderson, 1993). In this context, MDCK cells showing the polarized distribution of deep caveolae (Scheiffele et al., 1998) appear to be a good model system to study.

The number of shallow caveolae is equivalent to that of deep ones in many cell types (R. Nomura and T. Fujimoto, unpublished data). The prevalence of shallow caveolae could explain some of the conflicting results obtained by different experimental methods (Sargiacomo et al., 1993; Schnitzer et al., 1995; Smart et al., 1995; Song et al., 1996; Nomura et al., 1997). In conventional ultrathin sections, because it is difficult to distinguish shallow caveolae from simple plasmalemmal undulations, only deep invaginations can be identified definitely. Also only the deep ones were isolated by the colloidal silica-coating technique (Schnitzer et al., 1995), which takes advantage of the narrow orifice unpenetrable by the colloidal particles. On the other hand, by biochemical methods utilizing various chemical and/or physical perturbations (Sargiacomo et al., 1993; Smart et al., 1995; Song et al., 1996), both deep and shallow caveolae and other

detergent-insoluble membranes may be obtained in the same fraction (Kurzchalia et al., 1995; Simons and Ikonen, 1997). Therefore, we think that the first two methods and the latter ones give different results with respect to whether shallow caveolae are included. Freeze-fracture immunoelectron microscopy is unique in that deep and shallow caveolae can be identified and analyzed separately.

The α and β isoforms of caveolin-1 can be generated by alternative translation initiation (Scherer et al., 1995), but we recently found a mRNA encoding only the β isoform and the ratio of the two isoforms may be regulated at the transcription level (Kogo and Fujimoto, 2000). The present result suggests that the ratio of caveolin-1 isoforms is related to the differentiation of the caveolar structure. The biochemical basis of the morphological and possibly functional difference between the two isoforms is an important subject for future investigation.

We are grateful to Mr Kouei Sudoh, Ms Fujie Miyata, Ms Yukiko Takahashi, Mr Tetsuo Okumura and Ms Kumi Tauchi for excellent technical and secretarial assistance. This work was supported by Grants-in-Aid for Scientific Research of the Ministry of Education, Science, Sports and Culture of the Japanese Government and a research grant from Uehara Memorial Foundation.

REFERENCES

Anderson, R. G. W. (1993). Caveolae: where incoming and outgoing messengers meet. *Proc. Natl. Acad. Sci. USA* **90**, 10909-10913.

Anderson, R. G. W. (1998). The caveolae membrane system. *Annu. Rev. Biochem.* **67**, 199-225.

Couet, J., Li, S., Okamoto, T., Ikezu, T. and Lisanti, M. P. (1997). Identification of peptide and protein ligands for the caveolin-scaffolding domain. Implications for the interaction of caveolin with caveolae-associated proteins. *J. Biol. Chem.* **272**, 6525-6533.

Das, K., Lewis, R. Y., Scherer, P. E. and Lisanti, M. P. (1999). The membrane-spanning domains of caveolins-1 and -2 mediate the formation of caveolin hetero-oligomers. Implications for the assembly of caveolae membranes in vivo. *J. Biol. Chem.* **274**, 18721-18728.

Fielding, C. J., Bist, A. and Fielding, P. E. (1997). Caveolin mRNA levels are up-regulated by free cholesterol and down-regulated by oxysterols in fibroblast monolayers. *Proc. Natl. Acad. Sci. USA* **94**, 3753-3758.

Fra, A. M., Williamson, E., Simons, K. and Parton, R. G. (1995). De novo formation of caveolae in lymphocytes by expression of VIP21-caveolin. *Proc. Natl. Acad. Sci. USA* **92**, 8655-8659.

Fujimoto, K. (1995). Freeze-fracture replica electron microscopy combined with SDS digestion for cytochemical labeling of integral membrane proteins. Application to the immunogold labeling of intercellular junctional complexes. *J. Cell Sci.* **108**, 3443-3449.

Fujimoto, T. and Fujimoto, K. (1997). Metal sandwich method to quick-freeze monolayer cultured cells for freeze fracture. *J. Histochem. Cytochem.* **45**, 595-598.

Fujimoto, T., Hagiwara, H., Aoki, T., Kogo, H. and Nomura, R. (1998). Caveolae: a morphological point of view. *J. Electron Microsc.* **47**, 451-460.

Fujimoto, T., Hayashi, M., Iwamoto, M. and Ohno-Iwashita, Y. (1997). Crosslinked plasmalemmal cholesterol is sequestered to caveolae: analysis with a new cytochemical probe. *J. Histochem. Cytochem.* **45**, 1197-1205.

Fujimoto, T., Lee, K., Miwa, S. and Ogawa, K. (1991). Immunocytochemical localization of fodrin and ankyrin in bovine chromaffin cells in vitro. *J. Histochem. Cytochem.* **39**, 1485-1493.

Glenney, J. R., Jr. and Soppet, D. (1992). Sequence and expression of caveolin, a protein component of caveolae plasma membrane domains phosphorylated on tyrosine in Rous sarcoma virus-transformed fibroblasts. *Proc. Natl. Acad. Sci. USA* **89**, 10517-10521.

Hailstones, D., Sleer, L. S., Parton, R. G. and Stanley, K. K. (1998). Regulation of caveolin and caveolae by cholesterol in MDCK cells. *J. Lipid Res.* **39**, 369-379.

Kogo, H. and Fujimoto, T. (2000). Caveolin-1 isoforms are encoded by distinct mRNAs. Identification of of mouse caveolin-1 mRNA variants caused by alternative transcription initiation and splicing. *FEBS lett.* **465**, 119-123.

Kurzchalia, T. V., Hartmann, E. and Dupree, P. (1995). Guilt by insolubility – does a protein's detergent-insolubility reflect a caveolar location? *Trends Cell Biol.* **5**, 187-189.

Li, S., Couet, J. and Lisanti, M. P. (1996a). Src tyrosine kinases, Galpha subunits, and H-Ras share a common membrane-anchored scaffolding protein, caveolin. Caveolin binding negatively regulates the auto-activation of Src tyrosine kinases. *J. Biol. Chem.* **271**, 29182-29190.

Li, S., Song, K. S., Koh, S. S., Kikuchi, A. and Lisanti, M. P. (1996b). Baculovirus-based expression of mammalian caveolin in Sf21 insect cells. A model system for the biochemical and morphological study of caveolae biogenesis. *J. Biol. Chem.* **271**, 28647-28654.

Mora, R., Bonilha, V. L., Marmorstein, A., Scherer, P. E., Brown, D., Lisanti, M. P., and Rodriguez-Boulan, E. (1999). Caveolin-2 localizes to the golgi complex but redistributes to plasma membrane, caveolae, and rafts when co-expressed with caveolin-1. *J. Biol. Chem.* **274**, 25708-25717.

Murata, M., Peranen, J., Schreiner, R., Wieland, F., Kurzchalia, T. V. and Simons, K. (1995). VIP21/caveolin is a cholesterol-binding protein. *Proc. Natl. Acad. Sci. USA* **92**, 10339-10343.

Nomura, R., Inuo, C., Takahashi, Y., Asano, T. and Fujimoto, T. (1997). Two-dimensional distribution of Gi2α in the plasma membrane: a critical evaluation by immunocytochemistry. *FEBS Lett.* **415**, 139-144.

Parolini, I., Sargiacomo, M., Galbiati, F., Rizzo, G., Grignani, F., Engelman, J. A., Okamoto, T., Ikezu, T., Scherer, P. E., Mora, R., Rodriguez-Boulan, E., Peschle, C. and Lisanti, M. P. (1999). Caveolin-2 localizes to the Golgi complex but redistributes to plasma membrane, caveolae, and rafts when co-expressed with caveolin-1. *J. Biol. Chem.* **274**, 25718-25725.

Parton, R. G. (1996). Caveolae and caveolins. *Curr. Opin. Cell Biol.* **8**, 542-548.

Rothberg, K. G., Heuser, J. E., Donzell, W. C., Ying, Y. S., Glenney, J. R. and Anderson, R. G. W. (1992). Caveolin, a protein component of caveolae membrane coats. *Cell* **68**, 673-682.

Sargiacomo, M., Scherer, P. E., Tang, Z., Kubler, E., Song, K. S., Sanders, M. C. and Lisanti, M. P. (1995). Oligomeric structure of caveolin: implications for caveolae membrane organization. *Proc. Natl. Acad. Sci. USA* **92**, 9407-9411.

Sargiacomo, M., Sudol, M., Tang, Z. and Lisanti, M. P. (1993). Signal transducing molecules and glycosyl-phosphatidylinositol-linked proteins form a caveolin-rich insoluble complex in MDCK cells. *J. Cell Biol.* **122**, 789-807.

Scheiffele, P., Verkade, P., Fra, A. M., Virta, H., Simons, K. and Ikonen, E. (1998). Caveolin-1 and -2 in the exocytic pathway of MDCK cells. *J. Cell Biol.* **140**, 795-906.

Scherer, P. E., Lewis, R. Y., Volonte, D., Engelman, J. A., Galbiati, F., Couet, J., Kohtz, D. S., van Donselaar, E., Peters, P. and Lisanti, M. P. (1997). Cell-type and tissue-specific expression of caveolin-2. Caveolins 1 and 2 co-localize and form a stable hetero-oligomeric complex in vivo. *J. Biol. Chem.* **272**, 29337-29346.

Scherer, P. E., Okamoto, T., Chun, M., Nishimoto, I., Lodish, H. F. and Lisanti, M. P. (1996). Identification, sequence, and expression of caveolin-2 defines a caveolin gene family. *Proc. Natl. Acad. Sci. USA* **93**, 131-135.

Scherer, P. E., Tang, Z., Chun, M., Sargiacomo, M., Lodish, H. F. and Lisanti, M. P. (1995). Caveolin isoforms differ in their N-terminal protein sequence and subcellular distribution. Identification and epitope mapping of an isoform-specific monoclonal antibody probe. *J. Biol. Chem.* **270**, 16395-16401.

Schnitzer, J. E., McIntosh, D. P., Dvorak, A. M., Liu, J. and Oh, P. (1995). Separation of caveolae from associated microdomains of GPI-anchored proteins. *Science* **269**, 1435-1439.

Schnitzer, J. E., Oh, P. and McIntosh, D. P. (1996). Role of GTP hydrolysis in fission of caveolae directly from plasma membranes. *Science* **274**, 239-242.

Simons, K. and Ikonen, E. (1997). Functional rafts in cell membranes. *Nature* **387**, 569-572.

Smart, E. J., Ying, Y., Donzell, W. C. and Anderson, R. G. W. (1996). A role for caveolin in transport of cholesterol from endoplasmic reticulum to plasma membrane. *J. Biol. Chem.* **271**, 29427-29435.

Smart, E. J., Ying, Y. S., Mineo, C. and Anderson, R. G. W. (1995). A detergent-free method for purifying caveolae membrane from tissue culture cells. *Proc. Natl. Acad. Sci. USA* **92**, 10104-10108.

Song, S. K., Li, S., Okamoto, T., Quilliam, L. A., Sargiacomo, M. and Lisanti, M. P. (1996). Co-purification and direct interaction of Ras with caveolin, an integral membrane protein of caveolae microdomains. Detergent-free purification of caveolae microdomains. *J. Biol. Chem.* **271**, 9690-9697.

Tang, Z., Scherer, P. E., Okamoto, T., Song, K., Chu, C., Kohtz, D. S., Nishimoto, I., Lodish, H. F. and Lisanti, M. P. (1996). Molecular cloning of caveolin-3, a novel member of the caveolin gene family expressed predominantly in muscle. *J. Biol. Chem.* **271**, 2255-2261.

Vogel, U., Sandvig, K. and van Deurs, B. (1998). Expression of caveolin-1 and polarized formation of invaginated caveolae in Caco-2 and MDCK II cells. *J. Cell Sci.* **111**, 825-832.

Yamada, E. (1955). The fine structure of the gall bladder epithelium of the mouse. *J. Biophys. Biochem. Cytol.* **1**, 445-457.